SOOT FORMATION AND RADIATION IN TURBULENT JET DIFFUSION FLAMES UNDER NORMAL AND REDUCED GRAVITY CONDITIONS

Jerry C. Ku, Li Tong, and Jun Sun
Wayne State University
Detroit, Michigan 48202

Paul S. Greenberg
NASA Lewis Research Center
Cleveland, Ohio 44135

Devon W. Griffin
Sverdrup Technology, Inc.
Brook Park, Ohio 44142

Introduction

Most practical combustion processes, as well as fires and explosions, exhibit some characteristics of turbulent diffusion flames. For hydrocarbon fuels, the presence of soot particles significantly increases the level of radiative heat transfer from flames. In some cases, flame radiation can reach up to 75% of the heat release by combustion (ref. 1). Laminar diffusion flame results (ref. 2) show that radiation becomes stronger under reduced gravity conditions. Therefore, detailed soot formation and radiation must be included in the flame structure analysis. A study of sooting turbulent diffusion flames under reduced-gravity conditions will not only provide necessary information for such practical issues as spacecraft fire safety, but also develop better understanding of fundamentals for diffusion combustion.

Experimentally, full-field laser light transmission and thermophoretic soot particle sampling techniques will be used to measure flame soot particulate size and number density. Flame temperature will be measured using full-field two-color pyrometry and fine-gage thermocouples. These experiments are conducted in a drop tower.

On modeling, the focus is on complete coupling of flame structure, soot formation, and radiation. The conserved scalar approach based on Favre-averaged governing equations, k-ε-g turbulence model, and an assumed probability density function is used to predict flow field and gaseous species mole fractions profiles (refs. 3 and 4). A soot formation model developed by Syed et al. (refs. 5 and 6) will be modified to predict soot particle volume fraction and number density. The energy equation is incorporated to provide a full coupling between flame structure and radiation. The radiative heat flux is calculated from the radiative transfer equation (RTE) for a finite axisymmetric cylindrical enclosure, which will be solved by the P_3 spherical harmonics approximation (ref. 7).

In this paper, a summary of the work to date and of future plans is reported.

Experimental Results

Experiments are conducted using a 2.2-second drop rig. The rig is now instrumented for thermophoretic soot particle sampling and full-field laser light transmission measurements. Thermocouple and two-color pyrometry measurement are planned. Details for experiments are reported in another paper in this workshop (ref. 8).

Results were collected for laminar flames first to validate our setup and procedure. The nozzle has a diameter of 1.7 mm. Propane and ethylene at 1.0 and 1.5 cc/sec are tested. Micrographs of soot aggregates in 1.5 cc/sec propane-air diffusion flames are shown in Fig. 1. The significant difference in aggregate size (or number of primary particles per aggregate) between normal and reduced gravity conditions is noted, and this has been observed for all fuel and flow rate combinations.

Fig. 2 shows the mean diameter of primary soot particles as a function of height above nozzle exit. The size distribution, deduced from more than 100 particles per sample, agrees well with the normal distribution and 95% of the population falls in ±10 nm range. Incipient soot particles are larger under 0-g. This seems to support the argument that incipient soot starts as liquid droplets, whose dynamics is affected by the relative dominance of surface tension. Under 0-g, the oxidation stage seems to be much weaker for the 1.5 cc/sec case, so flames may smoke (i.e., release soot particles). It is therefore concluded that rates of nucleation, growth, coagulation, and oxidation are very different between 1-g and 0-g. 0-g data are needed for determining these rate constants in models. Larger aggregate and primary particle sizes mean that radiation heat transfer is even more significant under 0-g (ref. 9).

The full-field laser light transmission experiment has been tested for a 1-g flame. Soot volume fraction for a section as tall as 4.5 cm was measured instantaneously using a CCD camera. Results agree well with point-by-point measurements.

Modeling of Turbulent Jet Diffusion Flame

Following the conserved scalar approach, the structure of an axisymmetric turbulent diffusion flame is modeled using Favre-averaged boundary layer flow equations for conservation of mass, momentum, and mixture fraction described by Bilger (ref. 10), and a k-ε-g turbulence model proposed by Lockwood and Naguib (ref. 11). The governing equations can be written in a general form as (refs. 12)

$$\frac{\partial}{\partial x}(\bar{\rho}\tilde{u}\phi)+\frac{1}{r}\frac{\partial}{\partial r}(r\bar{\rho}\tilde{v}\phi)=\frac{1}{r}\frac{\partial}{\partial r}\left(r\mu_{\mathit{eff},\phi}\frac{\partial\phi}{\partial r}\right)+S_{\phi}\ , \tag{1}$$

where ϕ = 1 (continuity), $\tilde{u}$ (axial velocity), $\tilde{f}$ (mixture fraction), k (turbulence kinetic energy), ε (turbulence dissipation), or g (mixture fraction variance). Favre-averaged (mass weighted) quantities are defined as $\tilde{\phi}=\overline{\rho\phi}/\bar{\rho}$, whereas an overbar represents conventional time-averaging. Details for $\mu_{\mathit{eff},\phi}$ (effective viscosity) and S_{ϕ} (source term) can be found in the references. Buoyancy effects will only be considered in the mean flow equation, neglecting buoyancy-turbulence interactions.

Assuming all instantaneous scalar properties are functions of the mixture fraction only, termed the state relationships, the Favre-averaged mean and variance of scalar properties can be determined from an assumed probability density function (pdf). The mixture fraction is described as the mass fraction of fuel atoms anywhere in the flame and by virtue of its definition it is invariant with chemical reaction (so it is a conserved scalar). This allows the fluid mechanics to be decoupled from chemical reactions, and it is a good approximation if the rate of chemical reaction is limited by turbulent mixing and not by chemical kinetics (i.e. fast chemistry at equilibrium) and the diffusivities of all species and heat are equal.

The system represented by Eq. (1) is solved using a block-tridiagonal code written by Chen (ref. 13). Major gaseous species concentrations are then calculated based on the state relationships constructed from thermodynamic equilibrium (adiabatic flame) calculations using STANJAN (ref. 14) and a β-pdf. This has been found accurate for nonluminous and fuel-lean regions of luminous flames, but fails for rich regions of luminous flames. For better accuracy, the laminar flamelet approach (refs. 15 and 16), with the state relationships constructed from laminar flame data, may be used.

Modeling of Soot Formation and Oxidation

Compared to gaseous specious, soot inception is a much slower reaction, and soot particles have very different diffusivities. In addition, soot particles are subjected to turbulent mixing, thermophoretic forces, and strong radiation heat transfer effects. The structure analysis outlined above has been extended to model soot formation and oxidation. Magnussen and Hjertager (ref. 17) introduced rate equation models for both nucleation (based on number density) and surface-growth (based on mass concentration) stages. They used an energy equation in the form of Eq. (1), with the source term for radiation, which is calculated using a two-flux model. Gore and Faeth (ref. 4) constructed state relationships for soot volume fractions from laminar flame data, and for temperature from equilibrium combustion calculation with a fixed fraction of chemical energy release lost by radiation. Kent and Honnery (ref. 18) found that the state-relationship approach for soot volume fractions may work in the top oxidation portion of the flame, where turbulent mixing dominates, but not the lower inception portion, where chemical kinetics dominates. They calculated the temperature from an energy equation with a radiation term of $[-\varepsilon\sigma(T^4 - T_\infty^4)/\ell]$.

It is believed that the rate-equation model approach is more accurate for predicting soot formation and oxidation. Kennedy et al. (refs. 19 and 20) applied Eq. (1) for soot volume fraction in laminar diffusion flames. The soot volume fraction source term was replaced by rate equation models derived for nucleation, growth, and oxidation with an assumed average number density. An energy equation similar to that in Kent and Honnery (ref. 18) was used. The model predicts peak soot volume fractions fairly accurately, but not their radial distributions. We adopt a two-equation model, derived by Moss et al. (ref. 6) and Syed et al. (ref. 5), for soot number density (N) and volume fraction (f_v). The model agrees well with measured flat (Wolfhard-Parker) diffusion flame data. The model has been modified (ref. 21) to couple with reduced

chemical reaction mechanisms, and successfully predicted radiation heat transfer from a turbulent reacting jet in a cross-wind (ref. 22).

Since the model applies Eq. (1) to describe the transport of soot particles in terms of Favre-averaged number density and volume fraction, it can be easily incorporated into the reacting turbulent free-shear flow code. Rate equation models, representing nucleation, surfaced growth, coagulation, and oxidation, are used in source terms as

$$S_\phi = \bar{\alpha} - \bar{\beta}\bar{\rho}^2\left(\frac{N}{\rho n_0}\right)^2 - n_0^{1/3}\bar{\chi}\bar{\rho}\left(\frac{\rho_s f_v}{\rho}\right)^{-1/3}\left(\frac{N}{\rho n_0}\right)^{4/3}, \quad \phi = \frac{N}{\rho n_0}; \tag{2}$$

$$S_\phi = n_0^{1/3}(\bar{\gamma} - \bar{\chi})\bar{\rho}\left(\frac{\rho_s f_v}{\rho}\right)^{2/3}\left(\frac{N}{\rho n_0}\right)^{1/3} - C_\delta\bar{\alpha}, \quad \phi = \frac{\rho_s f_v}{\rho}; \tag{3}$$

where $n_0 = 6\times10^{26}$ is Avogadro's number and ρ_s is the mass density of solid carbon (typically 1.8-2.0g/cm^3). The rate constants α, β, γ, and χ are modeled in terms of mixture density $\bar{\rho}$, activation temperatures T_α and T_γ, and fuel mole fraction X_c, as

$$\alpha = C_\alpha\bar{\rho}^2 T^{1/2} X_c \exp(-T_\alpha/T), \tag{4}$$

$$\beta = C_\beta T^{1/2}, \tag{5}$$

$$\gamma = C_\gamma\bar{\rho} T^{1/2} X_c \exp(-T_\gamma/T), \tag{6}$$

$$\chi = C_\chi T^{1/2} X_{ox} \exp(-T_\chi/T), \tag{7}$$

wherein coefficients and temperatures are determined from experimental data. In Eq. (7), $X_{ox} = X_{OH}$ if $f \geq 0.064$ (fuel-rich), and $X_{ox} = 0.045X_{O_2}$ if $f < 0.064$ (fuel-lean). The effective viscosities are given in the form of

$$\mu_{eff,\phi} = \frac{\mu_t}{\sigma_\phi} = \frac{\bar{\rho}C_\mu k^2/\varepsilon}{\sigma_\phi}, \tag{8}$$

where σ_ϕ are determined from experimental data and C_μ is the same as that for $\tilde{u}$.

Flame Radiation Heat Transfer Calculation

Radiation is fully coupled with flame structure analysis through an energy equation given in the form of Eq. (1) with $\phi = \tilde{H}$ (total enthalpy) and $S_\phi = -\nabla\cdot\vec{q}_{rad}$. Turbulence-radiation interactions are neglected. Gore et al. (ref. 23), using a multi-ray method to calculate the radiative heat flux $\vec{q}_{rad}$, showed that the coupled analysis predicts more accurately than the uncoupled one. However, their work neglected the scattering by soot particles, but accounted for the effects of turbulence-radiation interactions.

The radiative transfer equation (RTE) for axisymmetric finite cylindrical enclosures such as for jet diffusion flames can be expressed as (ref. 7)

$$\left[\frac{1}{\beta}\left(\xi\frac{\partial}{\partial r} - \frac{\eta}{r}\frac{\partial}{\partial\phi} + \mu\frac{\partial}{\partial z}\right) + 1\right] I(r,\theta,\phi,z) = (1-\omega)I_b[T(r,z)]$$

$$+\frac{\omega}{4\pi}\int_0^{2\pi}\int_0^{\pi} I(r,\theta,\phi,z)\,\Phi(\theta,\phi,\theta',\phi')\sin\theta'\,d\theta'\,d\phi' \ . \qquad (9)$$

Here, the subscript λ denoting spectral quantities has been left off, I is intensity (with subscript b for blackbody), β is the extinction coefficient, ω is the single scattering albedo, ξ,η, and μ are direction cosines, and Φ is the phase function. Both β and ω are functions of position (r, z) for axisymmetric diffusion flames.

Menguc and Viskanta (ref. 7) derived a solution using the P_3 spherical harmonics approximation with the delta-Eddington approximation for the phase function. For soot agglomerates, the phase function can be better approximated by a third order Legendre polynomial series (ref. 9) given as

$$\Phi(\theta,\phi,\theta',\phi') = 1+\sum_{n=1}^{3} a_n P_n(\cos\psi) \ , \qquad (10)$$

where ψ is the scattering angle and $\cos\psi = \xi\xi' + \eta\eta' + \mu\mu'$, and coefficients a_n are to be determined. Applying the spherical harmonics approximation, the model equations are obtained by employing the following integrations

$$\int_0^{2\pi}\int_0^{\pi} [\text{Equation (9)}]Y_n^{m^*}\sin\theta\,d\theta\,d\phi \ , \qquad (11)$$

for $n = 0, 1, \cdots N$ and $m = -n, -n+1, \cdots n$, with N being the order of the P_N approximation. The spherical harmonics Y_n^m (superscript * denotes the complex conjugate) can be replaced with multiples of direction cosines. Define the moments of intensity as

$$I_0(r,z) = \int_0^{2\pi}\int_0^{\pi} I(r,\theta,\phi,z)\sin\theta\,d\theta\,d\phi \ , \qquad (12a)$$

$$I_{ij\cdots k}(r,z) = \int_0^{2\pi}\int_0^{\pi} (\ell_i\,\ell_j\cdots\ell_k)\,I(r,\theta,\phi,z)\sin\theta\,d\theta\,d\phi \ , \qquad (12b)$$

where each of the direction cosines ℓ_i, ℓ_j, and ℓ_k is ξ,η, or μ . Physically, the zeroth moment is the total incident radiation, whereas the first moments are radiative heat fluxes along the coordinate axis. The divergence of radiative heat flux vector, which appears in the energy equation, can then be calculated from

$$\nabla\cdot\vec{q}_{rad} = \beta(1-\omega)\{4\pi I_b[T(r,z)] - I_0(r,z)\} \equiv S(r,z) \ . \qquad (13)$$

After some manipulations, results obtained from Eq. (11) can be combined into four coupled elliptical partial differential equations for I_0, I_{11}, I_{33}, and I_{13}. The model equation for is given as

$$\left[4B_3(\Gamma_{rr}+\Gamma_{zz}) + \frac{1}{r}(4B_3+7B_1)\Gamma_r + \frac{1}{r^2}(-16B_3+14B_1) + \frac{70}{3}B_2\tau^2\right]I_0 = -\frac{35}{3}\tau^2\frac{S}{\beta} + A_1 \ , \qquad (14)$$

where B's are functions of a_n and ω, $\tau = \beta r_0$, A_1 is a function of B, τ, I_{11}, I_{33}, and I_{13}, and Γ is the derivative operator. These model equations, together with 16 Marshak's boundary conditions derived for diffusely emitting and reflecting opaque boundary, are solved numerically using a solver called ELLPACK (ref. 24).

To incorporate radiation calculations into the overall flame structure analysis, there are two major difficulties to be overcome. First is that equations for the moment of intensity such as Eq. (14) are elliptical, whereas equations represented by Eq. (1) are parabolic. It seems impossible to solve both systems simultaneously. An alternative, which we are testing now, is to iterate between these two systems until the results numerically converged. The second difficulty is on modeling the spectral radiative properties for integrating the RTE over the spectral range. We will first follow the wide-band approach used by Song and Viskanta (ref. 25).

Preliminary Results and Discussion

We first tested the flame structure and soot formation/oxidation predictions against results in Kent and Honnery (ref. 18) for an ethylene-air turbulent diffusion flame (nozzle diameter $D = 3$ mm, exit velocity $U_0 = 52$ m/sec, $Re_D = 9615$). Good agreement was found for mixture fractions. Fig. 3 shows the comparison for the temperature along the centerline and radially at $x/x_m = 0.4, 0.7$ ($x_m = 115D$). The dashed curve is from adiabatic combustion calculation, and the solid curve from a correction (ref. 21)

$$T = T_{ad}\left[1 - \beta\left(\frac{T_{ad}}{T_{max}}\right)^4\right], \tag{15}$$

where T_{ad} is the adiabatic temperature, T_{max} is the maximum adiabatic temperature, and $0.09 < b < 0.15$. Even Eq. (15) still over-predicts at the flame tip and outer edge. This demonstrates the importance of including the energy equation and detailed radiation heat transfer calculations.

Fig. 4 shows that the soot formation/oxidation model predicts soot volume fraction accurately. The over-prediction near the outer edge is caused by that of temperature. Fig. 5 shows the temperature and soot volume fraction contours, calculated using the same rate coefficients, for one of our test conditions ($Re_D = 536$, $Re_L \approx 7400$). The temperature contour shows a much taller and wider 0-g flame, as expected. The 0-g flame soot volume fraction contour is obviously unreasonable, since different rate constants are needed as concluded from laminar flame data. A reasonable prediction is possible by decreasing the level of oxidation for 0-g, which agrees with laminar flame results. 0-g measurements are needed for determining the rate constants.

The implementation of a iterative process between the RTE and the flame structure solvers has not been completed. Some numerical problems have been experienced, which are believed to be caused by zero β in part of the cylindrical enclosure where there is no flame. Fig. 6 shows the results of a forward calculation of the terms in the energy equation. Referring to Eq. (1) with $\phi = \tilde{H}$ and $S_\phi = -\nabla \cdot \tilde{q}_{rad}$, those two terms on the left are convection terms, and the first term on the right is conduction with the last term being radiation. The first three terms are calculated using total enthalpy from the adiabatic combustion calculation for 1-g. The last term is calculated using the temperature from Fig. 5 with an assumed uniform soot volume fraction of 10^{-8}. It is clear that all these terms are of about the same magnitude, and the radiation

term depends strongly on location. This confirms the importance of incorporating detailed radiation calculation into the flame structure analysis.

The modeling can be improved by accounting for interactions between turbulence and radiation (refs. 12 and 25), and between turbulence and buoyancy (ref. 22). The latter should be an important factor between 1-g and 0-g conditions.

Acknowledgments

The authors are indebted to J.-Y. Chen of UC/Berkeley for providing the solver code for turbulent reacting free-shear flows and John Roma of Baldwin Wallace College for electron microscopy and size analysis works.

References

1. H. A. Becker and D. Liang, "Soot Emission, Thermal Radiation, and Laminar Instability of Acetylene Diffusion Flames," Comb. Flame, Vol. 52, 247-256, 1983.
2. R. B. Edelman, M. Y. Bahadori, S. L. Olson, and D. P. and Stocker, "Laminar Diffusion Flames Under Micro-Gravity Conditions," AIAA-88-0645, AIAA 26th Aerospace Sciences Meeting, Reno, Nevada, 1988.
3. S.-M. Jeng and G. M. Faeth, "Species Concentrations and Turbulent Properties in Buoyant Methane Diffusion Flames," J. Heat Transfer, Vol. 106, 721-727, 1984.
4. J. P. Gore and G. M. Faeth, "Structure and Spectral Radiation Properties of Turbulent Ethylene/Air Diffusion Flames," 21st Symp. (Int.) Comb., 1521-1531, 1986.
5. K. J. Syed, C. D. Stewart, and J. B. Moss, "Modeling Soot Formation and Thermal Radiation in Buoyant Turbulent Diffusion Flames," 23rd Symp. (Int.) Comb., 1533-1541, 1990.
6. J. B. Moss, C. D. Stewart, and K. J. Syed, "Flow field Modeling of Soot Formation at Elevated Pressure," 22nd Symp. (Int.) Comb., 413-423, 1988.
7. Menguc, M. P., and Viskanta, R., 1986, "Radiative Transfer in Axisymmetric, Finite Cylindrical Enclosures," J. Heat Transfer, Vol. 108, 271-276.
8. D. Griffin and P. S. Greenberg, "Selected Microgravity Combustion Diagnostics Techniques," 2nd Int. Microgravity Comb. Workshop, Cleveland, Ohio, 1992.
9. J. C. Ku and K.-H. Shim, "Optical Diagnostics and Radiative Properties of Simulated Soot Agglomerates," J. Heat Transfer, Vol. 113, 953-958, 1991.
10. R. W. Bilger, "Turbulent Jet Diffusion Flames," Prog. Energy Comb. Sci., Vol. 1, 87-109, 1976.
11. F. C. Lockwood and A. S. Naguib,, "The Prediction of the Fluctuations in the Properties of Free, Round-Jet Turbulent Diffusion Flames," Comb. Flame, Vol. 24, 109-124, 1975.
12. G. M. Faeth, S.-M. Jeng, and J. Gore, "Radiation from Fires," ASME HTD-Vol. 45 Heat Transfer in Fire and Combustion Systems, 137-151, 1985.

13. J.-Y. Chen, W. Kollmann, and R. W. Dibble, "Numerical Computation of Turbulent Free-Shear Flows Using a Block-Tridigonal Solver for a Staggered Grid System," 18th Annual Pittsburgh Conf. Modeling and Simulation, 1987.

14. W. C. Reynolds, "The Element Potential Method for Chemical Equilibrium Analysis: Implementation in the Interactive Program STANJAN," Department of Mechanical Engineering, Stanford University, 1986.

15. R. W. Bilger, "Reaction Rates in Diffusion Flames," Comb. Flame, Vol. 30, 277-284, 1977.

16. S. K. Liew, N. C. Bray, and J. B. Moss, "A Flamelet Model of Turbulent Non-Premixed Combustion," Comb. Sci. Tech., Vol. 27, 69-73, 1981.

17. B. F. Magnussen and B. H. Hjertager, "On Mathematical Modeling of Turbulent Combustion with Special Emphasis on Soot Formation and Combustion," 16th Symp. (Int.) Comb, 719-729, 1976.

18. J. H. Kent and D. Honnery, "Soot and Mixture Fraction in Turbulent Diffusion Flames," Comb. Sci. Tech., Vol. 54, 383-397, 1987.

19. I. M. Kennedy, W. Kollmann, and J.-Y. Chen, "A Model for Soot Formation in a Laminar Diffusion Flame," Comb. Flame, Vol. 81, 73-85, 1990.

20. I. M. Kennedy, W. Kollmann, and J.-Y. Chen, "Predictions of Soot in Laminar Diffusion Flames," AIAA Journal, Vol. 29, 1452-1457, 1991.

21. K. M. Leung, R. P. Lindstedt, and W. P. Jones, "A Simplified Reaction Mechanism for Soot Formation in Nonpremixed Flames," Comb. Flame, Vol. 87, 289-305, 1991.

22. M. Fairweather, W. P. Jones, and R. P. Lindstedt, "Predictions of Radiative Transfer from a Turbulent Reacting Jet in a Cross-Wind," Comb. Flame, Vol. 89, 45-63, 1992.

23. J. P. Gore, U.-S. Ip, and Y. R. Sivathanu, "Coupled Structure and Radiation Analysis of Acetylene/Air Flames," J. Heat Transfer, Vol. 114, 487-493, 1992.

24. J. R. Rice and R. F. Boisvert, Solving Elliptic Problems Using ELLPACK, Springer-Verlag, New York, 1985.

25. T. H. Song and R. Viskanta, "Interaction of Radiation with Turbulence: Application to a Combustion System," J. Thermophysics, Vol. 1, 56-62, 1987.

(a) 1-g flame, 40 mm HAB

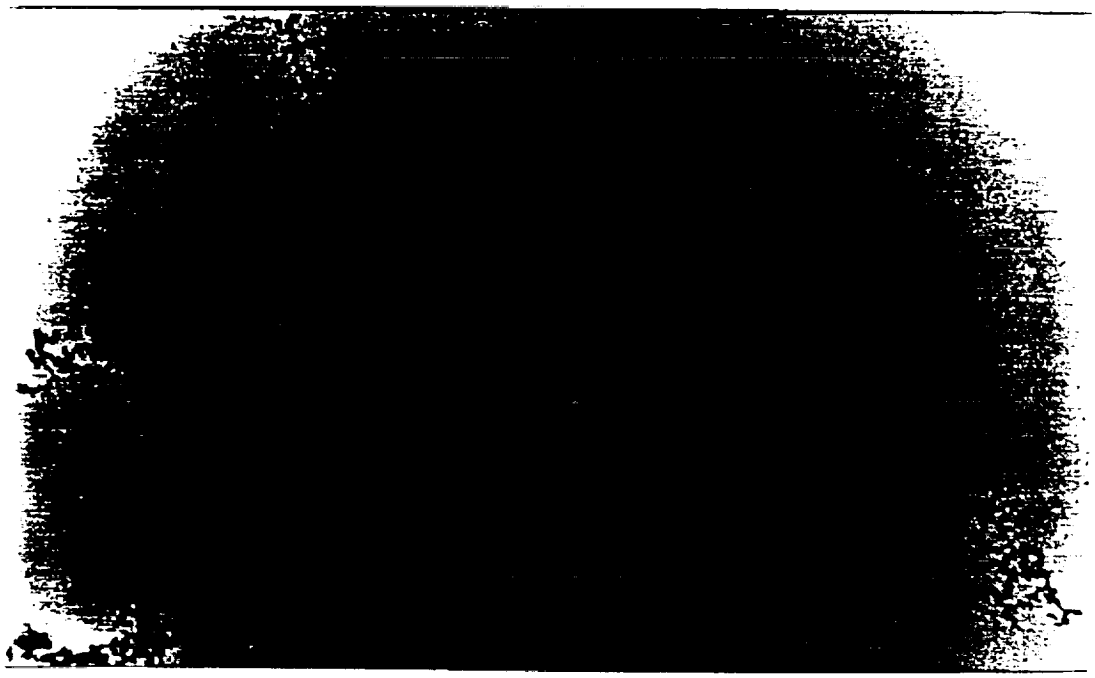

(b) 0-g flame, 80 mm HAB

Figure 1. Micrographs of soot aggregates in 1.5 cc/sec propane-air laminar diffusion flames under (a) normal, and (b) reduced gravity conditions. (1.7 mm nozzle dia.)

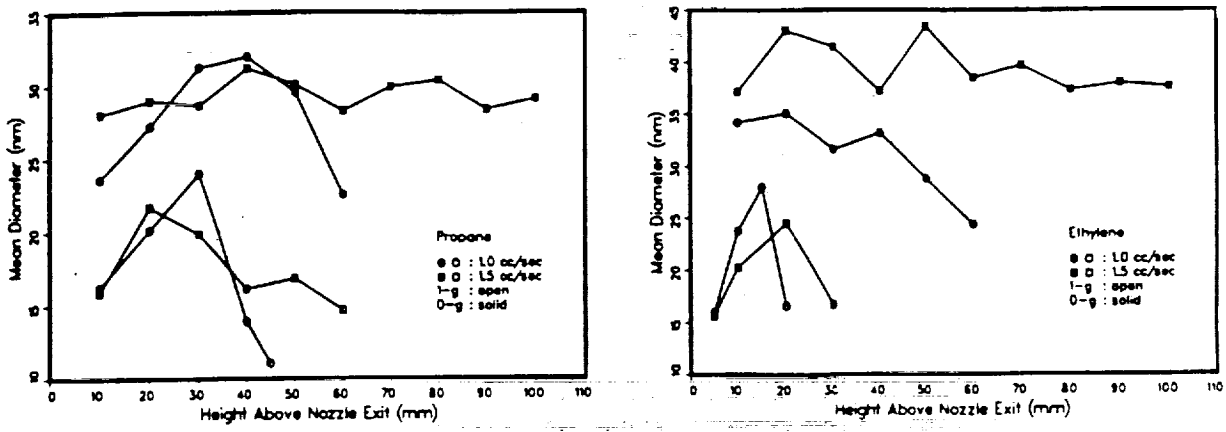

Figure 2. Mean diameter of primary soot particles in laminar diffusion flames.

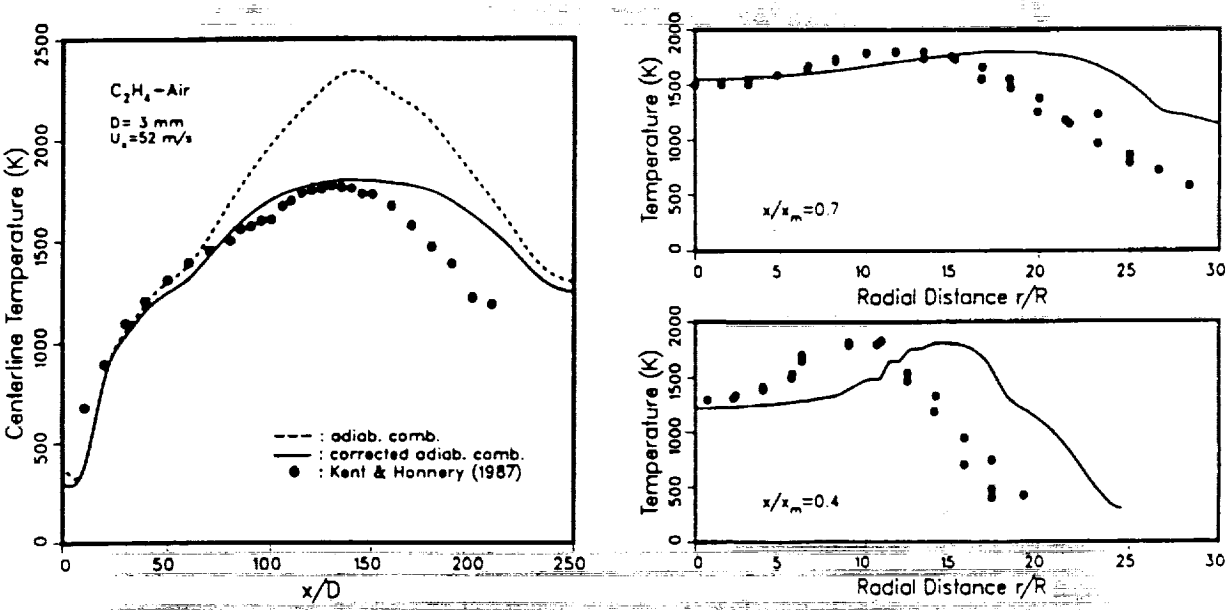

Figure 3. Comparisons of predicted and measured turbulent flame temperatures.

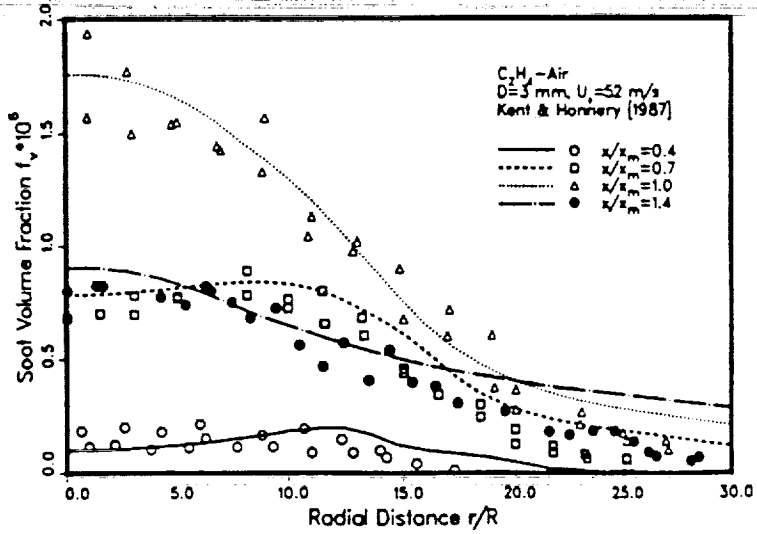

Figure 4. Predicted and measured turbulent flame soot volume fractions.

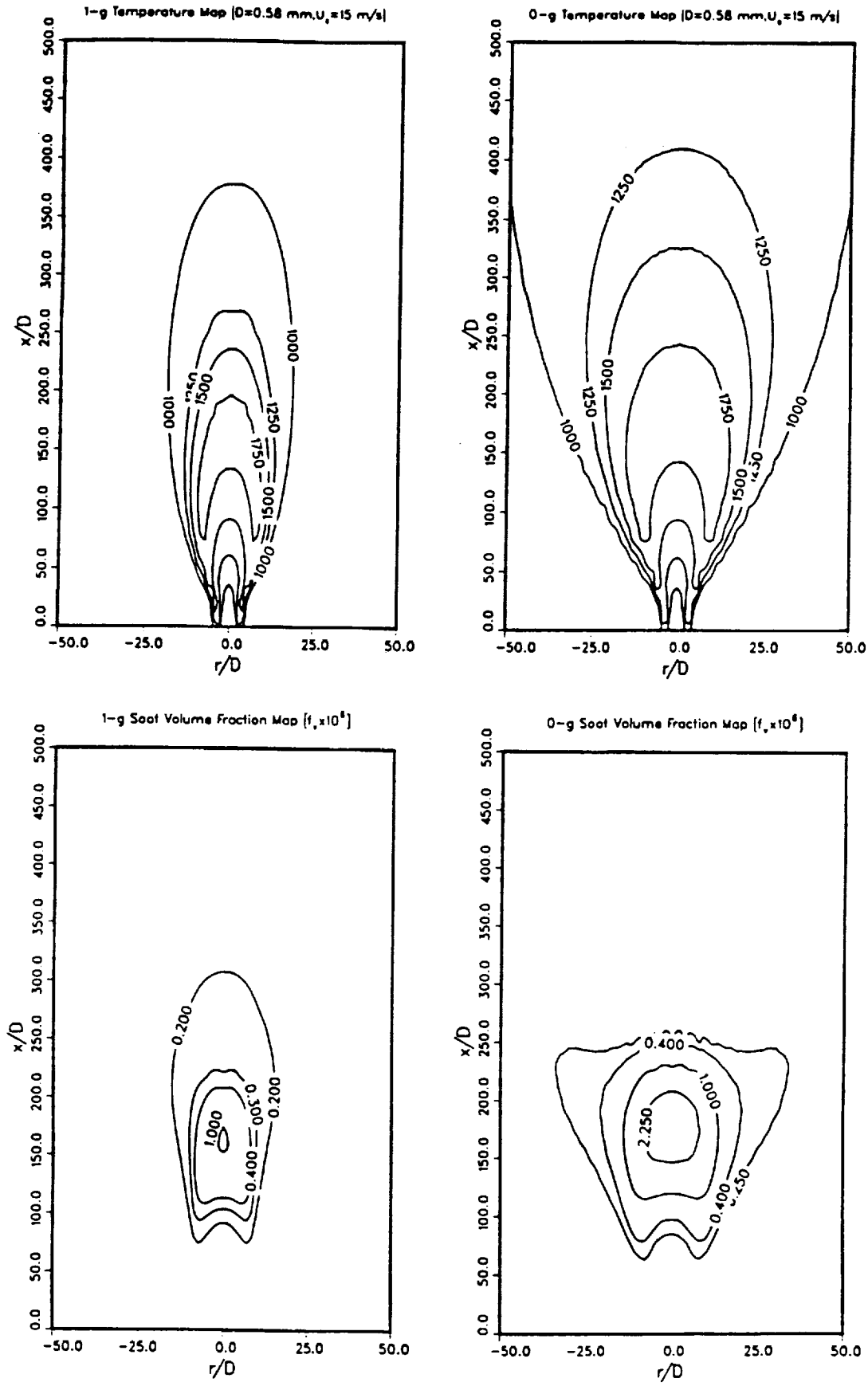

Figure 5. Normal- and reduced-gravity ethylene-air turbulent diffusion flames.

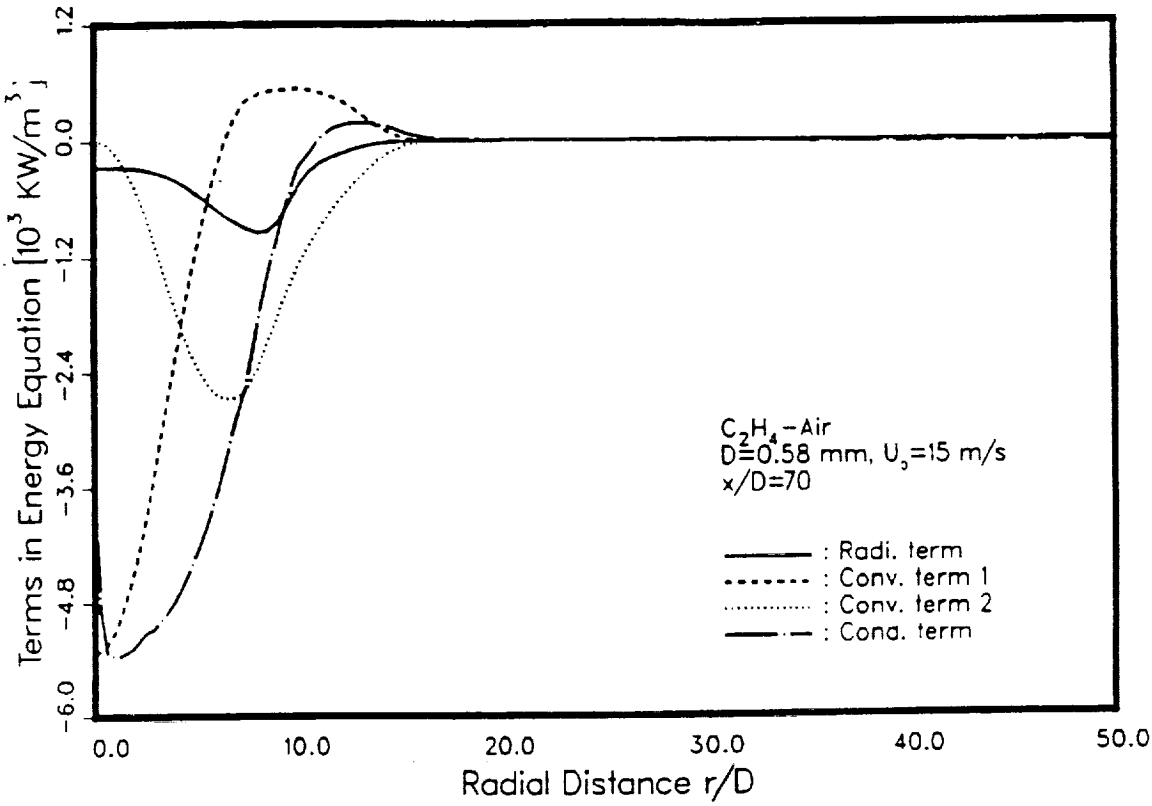

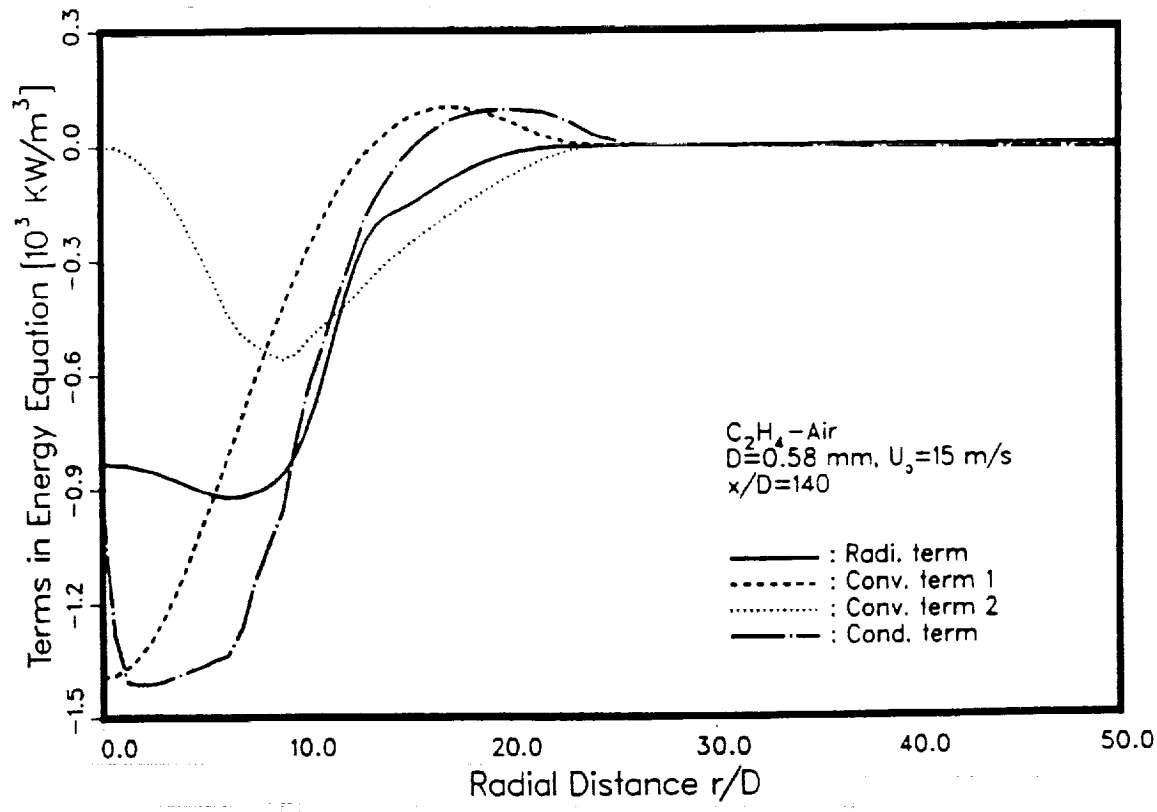

Figure 6. Estimated values of various terms in the energy equation with radiation.

COMMENTS

Question (J.P. Gore, Purdue University):

(1) What is the magnitude of turbulence-radiation interactions, and what is the justification for neglecting this effect in preference to scattering? Scattering is more important in optical diagnostics in the visible rather than in the thermal radiation term in energy equations.

(2) The effects of joint probability distribution functions between mixture fraction and enthalpy are important. Do you plan to model these?

(3) Are the soot volume fraction data from Kent and Honnery (1987) path-integrated equivalent measurements? If so, how is the comparison with predictions made?

(4) Chemical equilibrium calculations are not in agreement with measurements on the fuel-rich side. Should the model be improved in this aspect?

(5) In your verbal response you mentioned that there are other uncertainties such as refractive indices of soot. However, work reported in the literature has shown that items (1), (2) and (4) above have a very strong (even order of magnitude) influence on radiation heat loss. In my opinion, these need to be addressed with priority.

Answer: (1) There is no attempt at this point to model or estimate the magnitude of turbulence-radiation interaction, or to justify that it is negligible. The turbulence-radiation interaction is not included due to its complexity and the lack of definitive information about its effects. On the other hand, the scattering effects have been shown to be significant (Ref. 9) and can be dealt with in our radiation heat transfer calculations.

(2) We agree that the effects of joint pdf between mixture fraction and enthalpy are important and should be included in the model. However, this will not be our focus. Instead, we plan to follow works in existence, such as those by the commentator (Ref. 23), and those developed in the future.

(3) We believe that soot volume fraction data in Kent & Honnery (Ref. 18) are local values, instead of path-integrated. The last sentence in the second paragraph in Experimental Procedure states that horizontal traversing and Abel inversion were applied to extract local extinction data.

(4) Yes. We will improve this aspect of the model by using the laminar flamelet model, as indicated in the paper.

(5) One may argue that soot refractive index data are fairly accurate in the visible wavelengths, even though we are not perfectly convinced of that. However, it is fair to say that data in the infrared are highly questionable. Since there is no directly related analysis on the effects of this uncertainty, we plan to investigate this aspect more quantitatively.

Question: (Ivan Catton, UCLA): In transport processes, one is usually interested in number density and a mean diameter. Your electron micrographs show shapes as far from spherical, and one has to wonder what the "mean diameter" represents.

Answer: We consider soot particulates as aggregates of near-spherical primary particles. The shapes, as referred to in the question, are shapes of aggregates. The mean diameters, as referred to in the paper, are mean diameters of the near-spherical primary particles.